AD NUMBER

ADB383242

LIMITATION CHANGES

TO:

Approved for public release; distribution is unlimited.

FROM:

Distribution authorized to DoD and DoD contractors only; Administrative/Operational Use; JUN 2012. Other requests shall be referred to Naval Air Systems Command, Code 4.3.1, 48110 Shaw Road, Patuxent River, MD 20670-1906.

AUTHORITY

NAWCADPAX errata dtd 2 Jul 2013

NAVAL AIR WARFARE CENTER AIRCRAFT DIVISION
PATUXENT RIVER, MARYLAND

TECHNICAL REPORT

REPORT NO: NAWCADPAX/TR-2012/195

POTENTIAL CRASH LOCATION (PCL) MODEL

by

Natasha Bradley
Dr. David Burke

6 June 2012

DEPARTMENT OF THE NAVY
NAVAL AIR WARFARE CENTER AIRCRAFT DIVISION
PATUXENT RIVER, MARYLAND

NAWCADPAX/TR-2012/195
6 June 2012

POTENTIAL CRASH LOCATION (PCL) MODEL

by

Natasha Bradley
Dr. David Burke

RELEASED BY:

6 Jun 2012
ROLAND COCHRAN / AIR-4.3.1 / DATE
Systems Engineering Division
Naval Air Warfare Center Aircraft Division

REPORT DOCUMENTATION PAGE

Form Approved
OMB No. 0704-0188

1. REPORT DATE	2. REPORT TYPE	3. DATES COVERED
6 June 2012	Technical Report	June - November 2011

4. TITLE AND SUBTITLE Potential Crash Location (PCL) Model	5a. CONTRACT NUMBER 5b. GRANT NUMBER 5c. PROGRAM ELEMENT NUMBER PE064400D8Z
6. AUTHOR(S) Natasha Bradley Dr. David Burke	5d. PROJECT NUMBER 5e. TASK NUMBER 5f. WORK UNIT NUMBER
7. PERFORMING ORGANIZATION NAME(S) AND ADDRESS(ES) Naval Air Warfare Center Aircraft Division (AIR-4.3.1) 48110 Shaw Road Patuxent River, Maryland 20670-1161	8. PERFORMING ORGANIZATION REPORT NUMBER NAWCADPAX/TR-2012/195
9. SPONSORING/MONITORING AGENCY NAME(S) AND ADDRESS(ES) OUSD(AT&L)/S&TS-Unmanned Warfare Room 3B938 3090 Defense Pentagon Washington, DC 20301-3090	10. SPONSOR/MONITOR'S ACRONYM(S) 11. SPONSOR/MONITOR'S REPORT NUMBER(S)

12. DISTRIBUTION/AVAILABILITY STATEMENT

Distribution authorized to DOD and U.S. DOD contractors only; Administrative or Operational Use; June 2012. Other requests shall be referred to the Naval Air Systems Command (Code 4.3.1), 48110 Shaw Road, Patuxent River, Maryland 20670-1906

13. SUPPLEMENTARY NOTES

14. ABSTRACT

As the use of Unmanned Aerial Systems (UAS) grows, there is a need to integrate UAS into the National Airspace System. One challenge that has been encountered is developing a comprehensive risk analysis approach to model the risk posed by UAS operations to the general public. One component of this Target Level of Safety approach is a model for determining crash location. There are multiple approaches for modeling the potential crash locations of an UAS after a catastrophic failure. This report examines two potential models for fixed wing based on previous research into UAS risk analysis: the Clothier model (reference 1) and the Sensis model (reference 2) as well as two models for rotary wing aircraft.

15. SUBJECT TERMS

Potential Crash Location (PCL); Unmanned Aerial System (UAS); Clothier model; Sensis model

16. SECURITY CLASSIFICATION OF:			17. LIMITATION OF ABSTRACT	18. NUMBER OF PAGES	19a. NAME OF RESPONSIBLE PERSON
a. REPORT	b. ABSTRACT	c. THIS PAGE			19b. TELEPHONE NUMBER (include area code)
Unclassified	Unclassified	Unclassified	SAR	22	Dr. David Burke (301) 342-2185

Standard Form 298 (Rev. 8-98)
Prescribed by ANSI Std. Z39-18

SUMMARY

As the use of Unmanned Aerial Systems (UAS) grows, there is a need to integrate UAS into the National Airspace System. One of the critical requirements for expanding the operational area of UAS is to understand the risk to uninvolved third parties on the ground posed by the crash of a UAS. In order to address this issue Office of Secretary of Defense (OSD), Strategic and Tactical Systems – Unmanned Warfare Office, Air Worthiness IPT has sponsored the Target Level of Safety to Third Parties program. The objective of this program is to define a consistent calculation method to determine the relationship between UAS reliability, potential to cause damage and where it flies. Naval Air Systems Command, AIR 4.3.1 has lead the effort to develop this methodology. The Target Level of Safety (TLS) Program includes 5 modules; Casualty Expectation, Probability of Loss of Aircraft, Potential Crash Location, Lethal Crash Area and Population Density. This paper focuses on methods to define the Potential Crash Location of a UAS given a catastrophic failure.

There are multiple approaches for modeling the potential crash locations of an UAS after a catastrophic failure. This report examines two potential models for fixed wing aircraft based on previous research into UAS risk analysis: the Clothier model (reference 1) and the Sensis model (reference 2). Clothier uses a high fidelity dynamic model of a generic aircraft, while Sensis Inc. demonstrates a worst-case/best-case approach to defining the outer limits. This report also discusses two different approaches to modeling rotor craft UAS crash locations.

Contents

INTRODUCTION

BACKGROUND

As the use of Unmanned Aerial Systems (UAS) grows, there is a need to integrate UAS into the National Airspace System. One challenge that has been encountered is developing a comprehensive risk analysis approach to model the risk posed by UAS operations to the general public. The current effort is examining a Target Level of Safety (TLS) approach to modeling this risk to third parties, those not involved with UAS operations. One component of this TLS approach is a model for determining crash location. The Potential Crash Location (PCL) model uses some simplified equations to model the situation where an UAS has a catastrophic failure at some altitude. It provides the footprint within which the Unmanned Aircraft (UA) is most likely to crash. The model takes into account both fixed wing and rotor wing aircraft of various configurations and sizes. The Lethal Crash Area (LCA) model provides a method for calculating how large the actual lethal area at the site of impact would be. The LCA model is described in a separate report (reference 3).

There are several published approaches for modeling the potential crash locations of an UAS after a catastrophic failure. This report examines two potential models for fixed wing aircraft based on previous research into UAS risk analysis: the Clothier model (reference 1) and a Sensis model (reference 2). Clothier uses a high fidelity dynamic model of a generic aircraft, while Sensis Inc. demonstrates a worst-case/best-case approach to defining the outer limits. Both of these models are confined to fixed wing aircraft. This report also discusses two different approaches to modeling rotor craft UAS crash locations.

CLOTHIER MODEL

Clothier (reference 1) uses a 6-degree of freedom (6-DOF) model to find the footprint boundaries for gliding decent using differing aircraft parameters. Clothier uses a simple 6-DOF model to find the maximum extent of the crash footprint boundaries. Clothier first makes some assumptions to simplify the equations of motion. Since the aircraft is a UAS, it is safe to assume that it has coordinated flight. Clothier also assumes that the transitions between trim states are instantaneous. Therefore, the trajectories this model generates represent an upper bound on the actual trajectories that can be achieved. The model also assumes simple wing geometry, constant descent velocity, balanced flight (lift force equals weight), and no wind effects. The outer edge of the footprint is obtained by simulating a glide descent over all heading angles where a heading of 0 deg corresponds to an impact directly in front of the aircraft. Note however that a heading of 180 deg does not correspond to an impact point directly behind the aircraft due to a non-negligible turn radius. Therefore, Clothier assumes that the descent trajectory comprises a turn followed by a straight line glide. In regards to this turn, Clothier also assumed that there is a constant flight path angle (FPA) and the bank angle is 45 deg. He verified the assumption of a 45 deg bank angle by checking the displacement of the ground impact point given identical initial conditions; a 45 deg bank angle gives an approximately equal displacement. Clothier also made some assumptions that made the mathematics manageable such as rigid body dynamics, small

angle of attack (AOA), small thrust angle, and small FPA. A key assumption is that the entire flight will occur at sea level standard day. This assumption greatly simplifies the equations since varying atmospheric density would require flight by flight model rather than a generic model. This assumption is acceptable for this tool since most of the UAS will be flying at fairly low altitudes and any UAS up at higher altitudes would have a shorter glide distance due to lower air density.

In order to find the maximum extent of the footprint boundary, the FPA is needed. That can be found using the above assumptions with the differential equations for velocity and FPA (γ). The differential equations are (reference 1):

$$\left\|\dot{\tilde{V}}_w\right\| = \frac{g}{\left\|\widetilde{W}_h\right\|} \times \left[\left\|\tilde{T}_b\right\| \times \cos(\alpha + \varepsilon) - \left\|\widetilde{D}_w\right\| + \left\|\widetilde{W}_h\right\| \times \sin\gamma\right] = 0$$

$$\dot{\gamma} = \frac{g}{\left\|\widetilde{W}_h\right\| \times \left\|\tilde{V}_w\right\|} \times \left[\left(\left\|\tilde{T}_b\right\| \times \sin(\alpha + \varepsilon) + \left\|\tilde{L}_w\right\|\right) \times \cos\mu - \left\|\widetilde{W}_h\right\| \times \cos\gamma\right] = 0$$

When simplified using the assumption of a gliding decent, the differential velocity would become:

$$\left\|\widetilde{D}_w\right\| - \left\|\widetilde{W}_h\right\|\gamma = 0$$

By substituting the drag force equation, the FPA would be:

$$\gamma = \frac{\frac{1}{2}\rho S C_D \times \left\|\tilde{V}_w\right\|^2}{\left\|\widetilde{W}_h\right\|}$$

The AOA given γ, V_w and simplifying differential equation for γ, shown above, would become:

$$\left\|\tilde{L}_w\right\| \cos\mu - \left\|\widetilde{W}_h\right\| = 0$$

The Coefficient of Lift (C_L) and Coefficient of Drag (C_D) can be simplified to the equations below:

$$C_L = C_{L\alpha_0} + C_{L\alpha}\alpha$$

$$C_D = C_{D0} + \frac{C_L^2}{\pi ARE}$$

The 6-DOF model parameters can be evaluated using the above equations.

It is important to note that the minimum value for γ is achieved when the aircraft flies at its maximum lift to drag ratio. That ratio is achieved at the minimum drag velocity:

$$V_{Min\,Drag} = \|\tilde{V}\|^* = \sqrt{\frac{2\|\widetilde{W}\|}{\rho S}}\left(\frac{1}{\pi AR\, EC_{D0}}\right)^{0.25}$$

In flying this maximum lift to drag ratio profile, the maximum gliding range is:

$$d_{max}(H) = \frac{H}{\tan(\gamma_{MIN})} \approx \frac{H}{\gamma_{MIN}} = H\frac{C_L}{C_D}\Big|_{MAX}$$

Next, Clothier evaluates his maximum boundary results by plugging in values from different fixed wing UAV's into the 6-DOF model. Clothier found that footprint area grows uniformly as the height above ground level increases. At low heights, the footprint is more like a pie slice and as the height increases the footprint looks more like an ellipse. The footprint shape and area also varies with different aircraft, mainly due to the difference in glide ratios. The better the aircraft's glide ratio, the larger the footprint area. Initial velocity is another factor that determines shape since the higher the velocity, the less circular the footprint becomes due to the limitation on bank angle. Glide velocity has the opposite effect of height such that the higher the glide velocity the more the footprint looks like a circular sector.

After validating the 6-DOF model, Clothier then works on a footprint approximation technique. Clothier uses the two half ellipses to model the basic shape of a footprint. The model is then used to approximate the extremities of the true footprint. This model is illustrated in Figure 1 (reference 1).

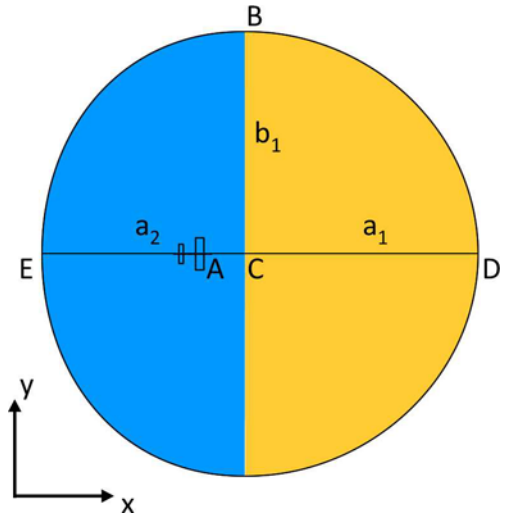

Figure 1: Illustration of dual half-ellipse geometric footprint primitive. Note that A is the initial aircraft location at the time of failure, AC is the turn radius rt for the chosen bank angle, CD = a1, CB = b1 = b2, EC = a2. C is the centre point for the frontal and back ellipse.

In Figure 1, A is the origin; E, B, and D are extremities. Thus, a_1, b_1, and a_2 can be used to approximate the extremities of the true footprint. C is the center of both ellipses, and C is distance r_t from A.

$$a_1 = maximum\ distance - r_t$$

$$b_1 = r_t + distance\ of\ glide$$

$$a_2 = r_t + distance\ of\ glide$$

To solve for a_1, b_1, and a_2, consider the front ellipse (yellow portion) b1 can be estimated with a descent trajectory comprising of a $\emptyset = 90°$ turn and glide. This trajectory is illustrated in Figure 2 (reference 1).

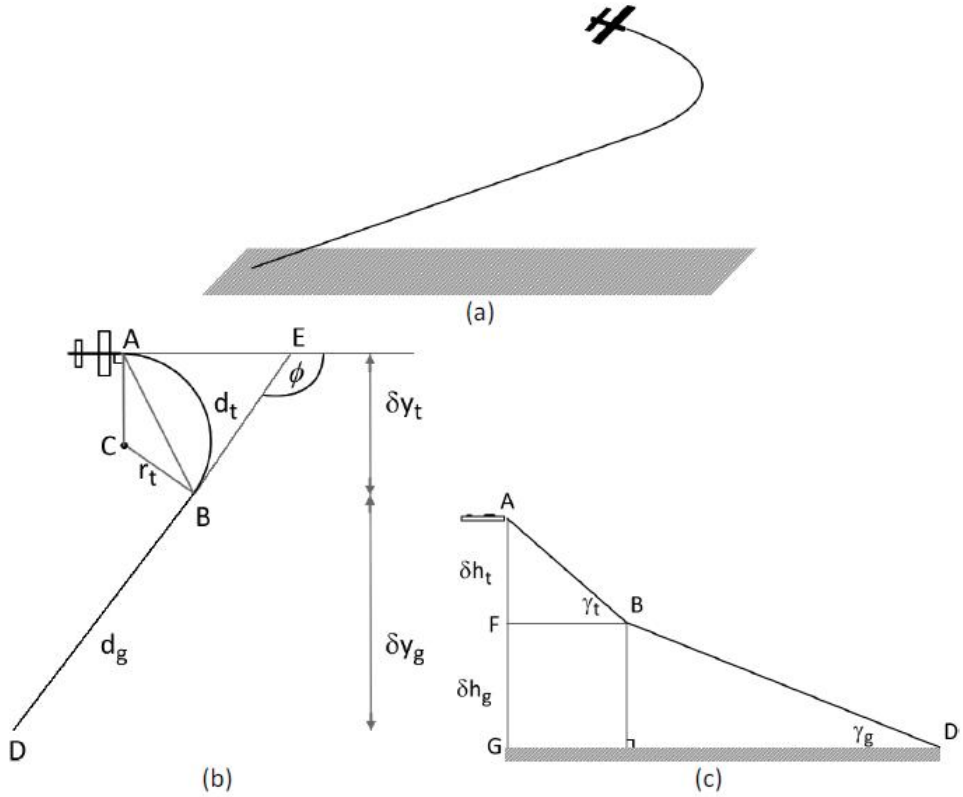

Figure 2: Illustration of geometric approximation of descent trajectory showing (a) 3D view, (b) top-down (xy plane) view, and (c) side-on view. This trajectory comprises a turn (modeled with a circular arc AB of radius rt), and a straight line glide BD. A constant FPA is assumed for the turn and similarly for the glide. AE and BE are tangential to the arc AB.

Using Figure 2 and assuming a level turn, you can approximate the turn radius:

$$r_t = \frac{V^2}{g \tan \mu}$$

Using Figure 2(b), it is possible to determine the distance traveled in the turn:

$$d_t = \emptyset r_t$$

Using Figure 2(c) of the illustration, it is possible to find AF = δh_t given AB = d_t assuming γ_t is a small angle:

$$\delta h_t = d_t \tan \gamma_t \approx d_t \gamma_t$$

Where γ_g is the FPA in the glide or the inverse of the maximum lift to drag ratio, FPA in the turn (γ_t) is:

$$\gamma_t = k_{tg} \gamma_g$$

Going back to the original assumptions, k_{tg} = 1.5 for a bank angle of 45 deg. Constant k_{tg} is determined empirically and enables accurate estimates of b_1 and a_2 which is shown below:

$$d_g = \frac{H - \delta h_t}{\tan \gamma_g} \approx \frac{H - \delta h_t}{\gamma_g}$$

$$b_1 = r_t + d_g$$

$$a_2 = r_t + d_g$$

$$a_1 = d_{Max} - r_t$$

This approximation only works for altitudes where a 90 deg turn is possible. Another method for finding b_1 is needed when $d_g \leq 0$. b_1 is an approximation of the maximum across track displacement. Using simple geometry, across track displacement due to the glide and due to the turn, for $0 \leq \emptyset \leq 90°$:

$$\delta y_g = d_g \sin \emptyset$$

$$\delta y_t = d_t \sin \frac{\emptyset}{2}$$

$$d_t = 2r \sin \frac{\emptyset}{2}$$

This means:

$$d_g = \frac{H - 2r\sin\frac{\emptyset}{2}\tan\gamma_t}{\tan\gamma_g}$$

$$\delta y = d_g \sin\emptyset + d_t \sin\frac{\emptyset}{2}$$

$$\delta y = \frac{H - 2r\sin\frac{\emptyset}{2}\tan\gamma_t}{\tan\gamma_g} + 2r\sin^2\frac{\emptyset}{2}$$

$$\delta y = \frac{H}{\tan\gamma_g}\sin\emptyset - \frac{2r\tan\gamma_t}{\tan\gamma_g}\sin\frac{\emptyset}{2}\sin\emptyset + 2r\sin^2\frac{\emptyset}{2}$$

Let $K_1 = \frac{H}{\tan\gamma_g}, K_2 = \frac{2r\tan\gamma_t}{\tan\gamma_g}$, and $K_3 = 2r$, to determine displacement find the differential of δy with respect to $\emptyset$. Then to determine if the displacement is a maximum find the second derivative of δy with respect to $\emptyset$. Clothier does an example of this and proves that the solution is a maximum. Therefore:

$$b_1 = \delta y$$

Given the above methods for finding a1, b1, and a2 (Figure 1), it is possible to find the total footprint area A:

$$A = \frac{\pi}{2}a_1 b_1 + \frac{\pi}{2}a_2 b_1$$

Clothier than validated empirically his approximation against the simulation results, He found that his method produced an accurate approximation of the true footprint extents (see reference 1) for the details on the simulation validation).

Clothier also found that, at low altitudes, the footprint area was more of a pie slice shape or a circular sector. This is due to the loss of altitude during the turn prohibiting the UA from reaching some areas behind it at the time of failure. The approximation for this pie shape crash location is provided in (reference 1).

SENSIS METHOD

Another method of finding the Crash Location Footprint for a fixed wing aircraft is the Sensis Method (reference 2). Instead of doing six differential equations to form a geometric shape, the Sensis group determines an outer edge and an inner edge to form the polygon. The outer edge of the footprint is limited by the maximum glide-down range of the aircraft; making sure to take into account the loss of altitude due to a heading change. The inner most edge of the polygon is

restricted by the turn radius of the vehicle, which is a function of the bank angle and speed. An example of this footprint can be seen in Figure 3 (reference 2).

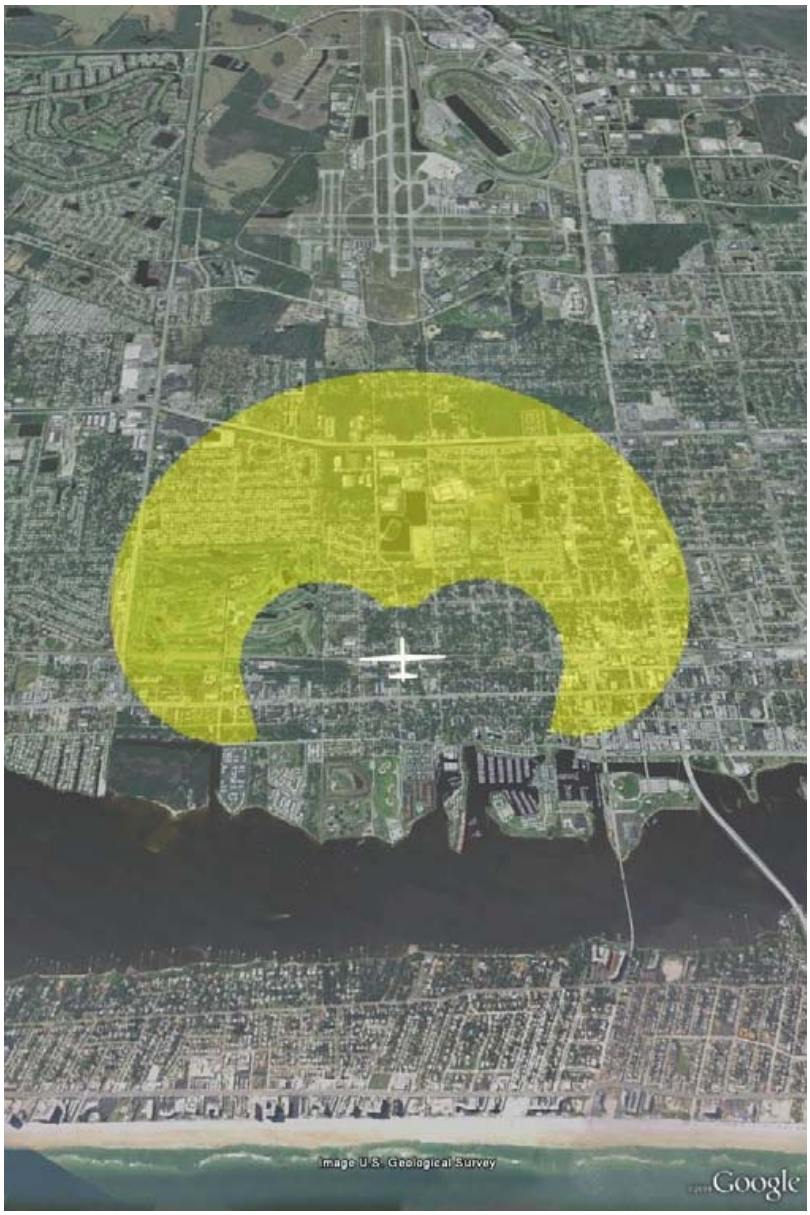

Figure 3: Sensis Method Crash Location Footprint

Although the Sensis method is another way of defining a crash footprint, there are reasons that it is not a good method for this effort. Primarily, this method focuses on the UAS operator finding a termination point, which implies that the failure is not catastrophic. That reasoning excludes the area immediately underneath the aircraft and behind the aircraft, which are logical locations where an UA could crash if there was a catastrophic failure. However, the Sensis method does

confirm some of the methodology used in Clothier's model in that the outer edge of the footprint is limited by the maximum glide-down range of the aircraft.

HELICOPTER MODEL

A search of published literature found no current helicopter model that can find the crash location using flight information and different types of crash trajectories. The two main assumptions that can be made for a helicopter crash is that there is no autorotation and drag is neglible[1]. With these assumptions the helicopter crash trajectory becomes projectile motion. This makes lift and drag negligible and also means that majority of the force of the crash will be straight down. Since the height and the speed of the UAS are already known the location of the crash can be determined using the following equation.

$$R = distance\ from\ Helicopter\ loss\ of\ control\ to\ Helicopter\ Crash\ site$$

$$g = 9.81 \frac{m}{s^2}\ (gravity)$$

$$V_0 = Helicopter\ Speed\ at\ loss\ of\ control$$

$$h = Helicopter\ Height\ at\ loss\ of\ control$$

$$R = V_0 \sqrt{\frac{2h}{g}}$$

HELICOPTER MODEL WITH AUTOROTATION

If the UAS has autorotation, this model changes drastically. The researchers investigated a method that can be used to apply autorotation to a UAS helicopter crash model (reference 3). This method states that gliding descent for helicopters rely on the lift generated by the rotors. Autorotation is the means of an unpowered rotor to maintain rotor RPM, lift, and control. The helicopter behaves such that the relative wind comes upward through the rotor disk. The aircraft is giving up altitude (or potential energy) at a controlled rate for kinetic energy to drive the rotor as shown in Figure 4 (reference 4).

[1] In reality, the tumbling helicopter would have very high and non-constant drag, but this assumption provides the most conservative estimate on how far the helicopter could go.

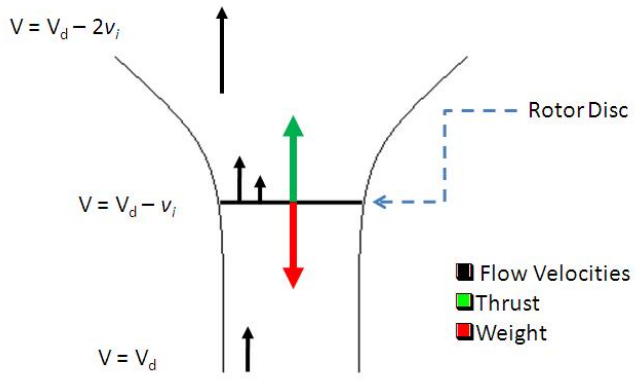

Figure 4: Momentum Theory of Autorotation through a Disc; Illustration by John Ball.

A simple way to model the autorotation for the large variety of shapes, sizes, and configurations of rotorcraft is with a momentum model (Figure 5, reference 4). The momentum model is presented by Leishman, Johnson, and Prouty (references 4, 5, and 6). A momentum theory solution states that the following assumptions are made: for axial flight (motion only in the vertical), the rotor disk can be modeled as an infinite number of blades and that the disk is strong enough to support pressure differences. As the rotorcraft descends, the relative flow field velocity far below the aircraft is the descent velocity. At the rotor disk, the velocity of the air is reduced by the downward velocity. This downward velocity is the hover induced velocity. This slows the airstream as it moves past the disk. Downstream of the rotor (which in this case in the up direction), the air separates and results in a relative velocity of the descent velocity minus twice the hover induced velocity.

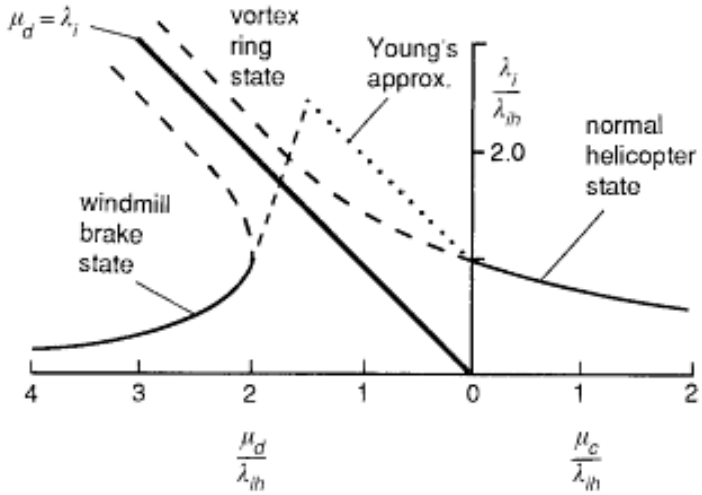

Figure 5: Solutions to Momentum Theory Autorotation and Young's Approximation

The physical solutions of this problem are complex and can be seen in the image above. Young approximated the ratio of descend velocity to induced hover velocity. Johnson built upon this and included an additional term, figure of merit. The result is a straightforward equation (reference 5).

$$FM = \frac{T\sqrt{T/2\rho A}}{P_{Hover\ Actual}}$$

Where FM represents the figure of merit and κ is the rotor efficiency. The figure of merit, as defined by Johnson is the ideal power required to hover over the actual power required. In a steady descent, the thrust can be approximated by the weight of the aircraft and the area as the area of the blades. If the power required for hover is not known, more advanced helicopter design should have figures of merit between 0.75 and 0.85 so a conservative assumption of 0.7 is used. Analysis shows that the figure of merit is significantly more influential in the value of the ratio of vertical descent velocity to hover induced velocity. Therefore, the model defines $\kappa = 1$, or an ideal rotor efficiency.

$$\frac{V_{D\ axial}}{V_i} = -\frac{\frac{1}{FM} - K}{1 + 3K} - \frac{7K}{1 + 3K}$$

The induced hover velocity can be calculated using equation:

$$V_i = \sqrt{\frac{T}{2\rho A}}$$

This process can help estimate the descent rate of a helicopter in axial flight conditions. Where p is the air density (assume constant sea level), T is the thrust, and A is the blade area.

Once the velocity of descent is known the distance traveled can easily be calculated by replacing gravity with the decent velocity or with the rate of decent velocity.

$$R = V_0\sqrt{\frac{2h}{V_i}}$$

TARGET LEVEL OF SAFETY MODEL TOOL

For the TLS model, some assumptions were made to simplify the calculation methods for PCL so that the calculations and the output could be performed by a tool built to use as few variables as possible. The Clothier method was chosen as the model for fixed wing aircraft. The tool uses glide ratio, aircraft max speed, and aircraft weight to do the necessary calculations. It was

decided for the TLS tool to implement both the ellipse and pie slice models and have the tool switch between the ellipse and pie slice patterns[2]. For helicopters, the assumption was made that autorotation was not an option based on the capabilities of current unmanned helicopters. Therefore, the tool will use the projectile model for all helicopter failures.

The crash location calculations are just one portion of the TLS tool, the other portion is LCA. Although the LCA is not important to the PCL area, and therefore not described in this paper, the crash location area does pull the operating velocity, and the max glide ratio from that portion of the tool. Figure 6 is a photo of the crash location area page in the TLS tool.

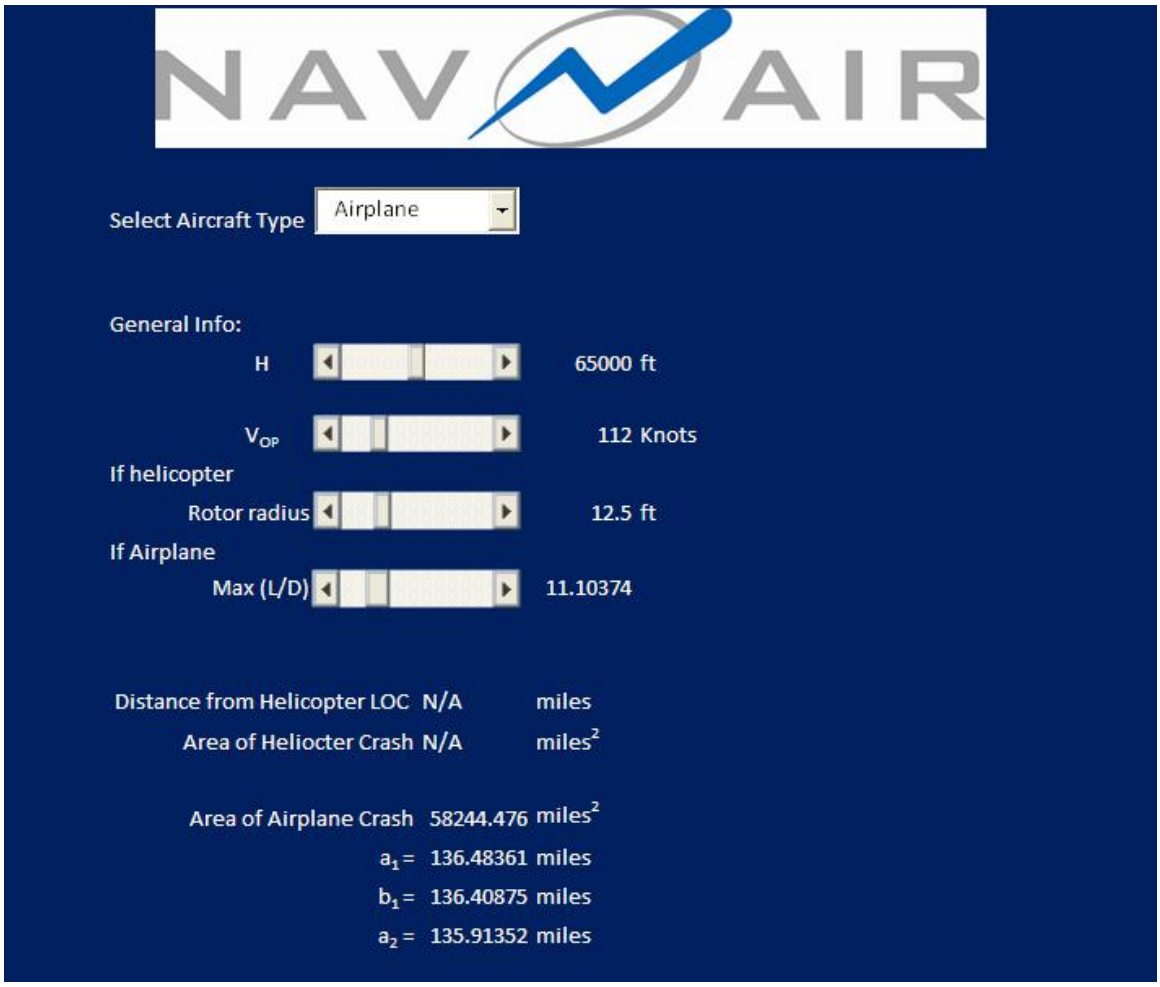

Figure 6: TLS Tool Crash Location Page

[2] The switching altitude depends on several aircraft parameters including airspeed and lift to drag ratio. It typically occurs around 50 to 100 ft AGL altitude although very fast aircraft maintain the pie slice model up to altitudes of ~1,000 ft. The exact algorithm for this switching is documented in the 3PRAT report.

THIS PAGE INTENTIONALLY LEFT BLANK

REFERENCES

1. Wu, Paul, Clothier, Reece and Walker, Rodney. *UAS Risk Assessment Tool Project: Risk Model Derivation.* s.l.: ARCAA, 2010.

2. Ford, Andrew and McEntee, Kevin. *Assesment of Risk to Ground Population due to an Unmanned Aircraft In-Flight Failure.* East Syracuse: Sensis, 2010.

3. NAWCAD Patuxent River Technical Report No. NAWCADPAX/TR-2012/196, Crash Lethality Model, of 6 Jun 2012.

4. Leishman, J. Gordon. *Principles of Helicopter Aerodynamics.* New York, NY: Cambridge University Press, 2006.

5. Johnson, Wayne. *Helicopter Theory.* Princeton, New Jersey: Princeton University Press, 1994.

6. Prouty, Raymond. *Helicopter Performance, Stability, and Control.* Malabar, Florida: Krieger Publishing Company, Inc., 1986.

THIS PAGE INTENTIONALLY LEFT BLANK

DISTRIBUTION:

NAVAIRSYSCOM (AIR-4.3.1 - Cochran), Bldg. 2187, Room 3358 (4)
48110 Shaw Road, Patuxent River, MD 20670-1906
NAVAIRSYSCOM (AIR-4.5 - Burke), Bldg. 2272, Room 253 (5)
47123 Buse Road, Patuxent River, MD 20670-1547
NAVAIRSYSCOM (AIR-4.6.2 - Knott), Bldg. 2187, Room 1280D5 (2)
48110 Shaw Road, Patuxent River, MD 20670-1906
NAVAIRSYSCOM (AIR-4.5.1 - Andrew), Bldg. 2187, Room 2242 (2)
48110 Shaw Road, Patuxent River, MD 20670-1906
NAVAIRWARCENACDIV (5.1.2.1 - Ball), Bldg. 111, Room 240 (2)
22755 Saufley Road, Patuxent River, MD 20670-1619
U.S. Army Research Laboratory (Bradley), Vehicle Technology Directorate (1)
4603 Flare Loop, Aberdeen Proving Grounds, MD 21005
NAVAIRWARCENACDIV (4.3.2.6 - Donley), Bldg. 2187, Room 1313 (1)
48110 Shaw Road, Patuxent River, MD 20670-1906
NAVAIRSYSCOM (AIR-4.10.3 - Polakovics), Bldg. 2187 (1)
48110 Shaw Road, Patuxent River, MD 20670-1906
NAVAIRWARCENACDIV (5.2.2G - Jacob), Bldg. 2118, Room 110 (1)
23013 Cedar Point Road, Patuxent River, MD 20670
NAVAIRSYSCOM (AIR-5.1G - Roberts), Bldg. 8010 (1)
47320 Priests Point Loop , St. Inigoes, MD 20684-4017
NAVAIRSYSCOM (UASTD - Heasley), Bldg. 8127 (1)
17637 Nesea Way, St. Inigoes, MD 20684-4015
NAVAIRSYSCOM (PEO U&W - Daniels), Bldg. 2272, Room 253 (1)
47123 Buse Road, Patuxent River, MD 20670-1547
NAVAIRSYSCOM (PEO U&W - Evans), Bldg. 2272, Room 246 (1)
47123 Buse Road, Patuxent River, MD 20670-1547
NAVAIRSYSCOM (AIR-4.1.6 - Zidzick), 235, Bldg. 4010, Room 235 (1)
48187 Standley Road, Patuxent River, MD 20670
NAVAIRSYSCOM (AIR-4.3D - Rubinsky), Bldg. 2187, Room 3322 (1)
48110 Shaw Road, Patuxent River, MD 20670-1906
NAVAIRSYSCOM (AIR-4.5.1 - Thorpe), Bldg. 2187, Room 2242 (1)
48110 Shaw Road, Patuxent River, MD 20670-1906
ARMY (RDMR-AEV - Flynn), 4488 Martin Road (1)
Redstone Arsenal, AL 35898
NAVAIRWARCENACDIV (AIR-4.0P - Adams), Bldg. 460, Room 222, (1)
22244 Cedar Point Road, Patuxent River, MD 20670-1163
NAVAIRDEVCENACDIV (AIR-5.0E - Rusher), Bldg. 1492, Room 24, (1)
47758 Ranch Road, Patuxent River, MD 20670-1456
WPAFB (ESC/ENSI - Rodreguez), Bldg. 28 (1)
Wright Patterson AFB, OH 45433
WPAFB (ABSSA/SIPT - Schaeffer), Area B, Bldg. 557, Room 005D (1)
Wright Patterson AFB, OH 45433

Pentagon (OUSD [AT&L]/S&TS-Unmanned Warfare - Greenly), Room 3B938 (1)
3090 Defense Pentagon, Washington, DC 20301-3090
NAVAIRWARCENACDIV (4.12.6.2), Bldg. 407, Room 116 (1)
22269 Cedar Point Road, Patuxent River, MD 20670-1120
DTIC (1)
8725 John J. Kingman Road, Suite 0944, Ft. Belvoir, VA 22060-6218

NAVAL AIR WARFARE CENTER AIRCRAFT DIVISION
PATUXENT RIVER, MARYLAND

ERRATA

ERRATA NUMBER: NAWCADPAX/RTR-2012/195E

DATE: 2 July 2013

FROM:
Commander, Naval Air Warfare Center Aircraft Division, Patuxent River, Maryland 20670-1161

TO:
Commander, Naval Air Systems Command Headquarters, 47123 Buse Road, Patuxent River, Maryland 20670-1547

REPORT NO.:	**DATE:**
NAWCADPAX/RTR-2012/195	6 June 2012

REPORT TITLE:
Potential Crash Location (PCL) Model

REQUEST THAT RECIPIENTS OF THE ABOVE REPORT INCORPORATE THE FOLLOWING CORRECTIONS:

Per Public Release Authorization Request No. 2013-591, make pen and ink change to Distribution statement to read:
Approved for public release; distribution is unlimited.

B383242

20120814182

DISTRIBUTION:	**RELEASED BY:**
Same as original document.	27 Jun 2013 ROLAND COCHRAN / 4.3.1 / DATE Air Vehicle Systems Engineering Division Naval Air Warfare Center Aircraft Division

Approved for public release; distribution is unlimited.